Progression of Flagellar Stages during Artificially Delayed Motility Initiation in Sea Urchin Sperm

Authors: Ohmuro, Junko, Mogami, Yoshihiro, and Baba, Shoji A.

Progression of Flagellar Stages during Artificially Delayed Motility Initiation in Sea Urchin Sperm

Junko Ohmuro*, Yoshihiro Mogami and Shoji A. Baba

Department of Biology, Ochanomizu University, Otsuka 2-1-1, Tokyo 112-8610, Japan

ABSTRACT—Transition from immotile to motile flagella may involve a series of states, in which some of regulatory mechanisms underlying normal flagellar movement are working with others being still suppressed. To address ourselves to the study of starting transients of flagella, we analyzed flagellar movement of sea urchin sperm whose motility initiation had been retarded in an experimental solution, so that we could capture the instance at which individual spermatozoa began their flagellar beating. Initially straight and immotile flagella began to shiver at low amplitude, then propagated exclusively the principal bend (P bend), and finally started stable flagellar beating. The site of generation of the P bend in the *P-bend propagating* stage varied in position in the basal region up to 10 μm from the base, indicating that the ability of autonomous bend generation is not exclusively possessed by the very basal region but can be unmasked throughout a wider region when the reverse bend (R bend) is suppressed. The rate of change in the shear angle, the curvature of the R bend and the frequency and regularity of beating substantially increased upon transition from *P-bend propagating* to *full-beating*, while the propagation velocity of bends remained unchanged. These findings indicate that artificially delayed motility initiation may accompany sequential modification of the motile system and that mechanisms underlying flagellar motility can be analyzed separately under experimentally retarded conditions.

Key words:　sea-urchin sperm, flagella, motility initiation, P-bend propagating, high-speed video

INTRODUCTION

Ciliary and flagellar motility depends on a series of cooperative interactions between the various components within the axoneme. Starting and stopping transients of motility and the transition between different states of activity have been investigated to functionally dissect these interactions (Miller, and Brokaw, 1970; Rikmenspoel, 1978; Goldstein, 1979; Gibbons and Gibbons, 1980b; Baba and Mogami, 1987a). Sea-urchin sperm cells are stored in a quiescent state in the gonads, but upon release into seawater, flagellar motility is initiated, and a 50-fold activation of respiration occurs (Christen *et al.*, 1982, 1983). Motility initiation involves the switching on of the sperm flagellar apparatus, which occurs simultaneously or successively, probably creating transient states of the axoneme with some mechanisms working but others being suppressed. Motility initiation, however, occurs instantaneously or so rapid that it is hard to capture such transients for analysis, when sperm are diluted in seawater (Clapper *et al.*, 1985; Dorsten *et al.*, 1997).

We developed a solution, which contains 100 mM K⁺, 2 mM EDTA and 900 mM glycine at pH 8.2, for use in the study of regulatory mechanisms of flagellar movement, which might be revealed during artificially delayed motility initiation. This solution, which will be referred to as KEG, substantially retards motility initiation in sea-urchin sperm cells as described later on. The idea of retardation by KEG is based on the facts that sea-urchin sperm remain quiescent in Na⁺-free seawater (Lee *et al.*, 1983; Bibring *et al.*, 1984; Schackmann *et al.*, 1984; Gatti and Christen, 1985; Christen *et al.*, 1986), and also immotile at elevated K⁺ concentrations (Christen *et al.*, 1986; Bracho *et al.*, 1997) and become active when the intracellular pH is elevated, e.g., by addition of Na⁺ or amine (Christen *et al.*, 1982; Lee *et al.*, 1983; Bibring *et al.*, 1984; Lee, 1984a, b; Bracho *et al.*, 1997), and that activation is, however, delayed in the presence of a variety of metal chelators including EDTA (Clapper *et al.*, 1985; Christen *et al.*, 1986). The KEG retardation of motility initiation first revealed distinct transient patterns of flagellar bending described in the present study. Transition events between these patterns were recorded on a high-speed video camera and were analyzed, although they occurred sporadically and within some ten milliseconds in individual cells.

* Corresponding author: Tel.　+81-3-5978-5714;
　　　　　　　　　　　　FAX. +81-3-5978-5368.
　　　　　　　　　　　　E-mail: jun425@cc.ocha.ac.jp

MATERIALS AND METHODS

Dry sperm

Dry sperm were obtained from the sea urchin, *Hemicentrotus pulcherrimus*, by injecting 0.55 M KCl into the body cavity after removal of the Aristotle's lantern. To get completely inactive sperm, the body fluid was discarded through the oral opening and then the remaining fluid, which otherwise oozed upon spawning, was removed by absorbent tissue. The dry sperm were stored in a refrigerator and used within 6 hours.

Solutions

Artificial seawater (ASW), 450 mM NaCl, 10 mM KCl, 10 mM CaCl₂, 25 mM MgCl₂, 28 mM MgSO₄, 10 mM Tris-HCl (pH 8.2), and KEG, 900 mM glycine, 60 mM KCl, 40 mM KOH and 2 mM EDTA (pH 8.2), were used. ASW and KEG contained 0.01% bovine serum albumin (Sigma) to prevent sperm flagella from attaching to the surface of cover glass.

Recording and analysis

Sperm diluted and mixed well in KEG or ASW in a test tube were immediately put in an observation chamber made of slide and cover glasses separated with 0.5-mm thick silicone rubber cut into a rectangular frame. Pictures just under the cover glass were recorded in a temperature-controlled box of 20°C, through an Olympus phase contrast microscope with a 20 × objective (BH2 with NH20, Olympus Co., Tokyo) using an NTSC-format video tape recorder (VTR, Victor SVHS HR-VX1, Victor Co., Tokyo) under illumination with xenon flash tubes driven by laboratory-made power controllers (Baba and Mogami, 1987b). Motile spermatozoa were discriminated from non-motile by comparing trajectories, which were made by means of image processing on a DIG98 image processor (Ditect Co., Tokyo) interfaced with a computer (PC). The average number of motile cells of four successive measurements at 5-s intervals was plotted as a percent motility relative to the maximum reached during individual episodes after dilution. Spermatozoa which propagate the principal bend (P bend) and the reverse bend (R bend) alternately in a manner usually found in those diluted in seawater were designated as "*full-beating*" ones, while spermatozoa propagating exclusively the P bend were referred to as "*P-bend propagating*" ones (for definition of bends, see Gibbons and Gibbons, 1972). The percentage of *full-beating* sperm and that of *P-bend propagating* relative to the motile were also measured respectively as above.

To evaluate bending forms quantitatively, sperm diluted in KEG or in ASW in a test tube were immediately put on a Millipore filter of 13 mm in diameter (HA, Nihon Millipore Ltd., Tokyo) with a hole of 5.5 mm punched through at the center. The layer of solution trapped in the central hole was made as thin as possible to enable us to bring the transient and hence otherwise elusive events into focus. This ring-shaped disk was placed at the center of a cover glass, which was then inverted and supported on a slide glass by a frame of 0.5-mm thick silicone rubber, which in turn formed the walls of a humidity chamber. Pictures of sperm just starting movements in the hanging drop flattened by the surface tension were recorded at room temperatures, through an Olympus phase contrast microscope with a 40 × objective (BH2 with NH40) using VTR or a high-speed video recorder (HSVTR, EktaPro HR1000, Kodak, Tokyo) under illumination with a power xenon flash tube (Miyake *et al.*, 1998). Individual flagellar images captured through the DIG98 image processor from VTR or HSVTR were tracked manually or automatically using flagellar image analysis software, Bohboh (BohbohSoft, Tokyo), on a PC. The angle of the tangent to the flagellar shaft measured with reference to the direction of the axis of sperm head, which will be referred to as shear angle, and the curvature of the shaft were computed as functions of time t and distance s along the flagellum measured from the base (Baba and Mogami, 1985). Based on the description of flagellar bending waves as "sine-generated" by Hiramoto and Baba (Hiramoto and Baba, 1978), the shear angle ϕ (s, t) was fitted using equations of the form:

$$\phi (s, t)=\phi_a(s) \cos \{(S_\phi (s)-2\pi ft)\}+\phi_b(s), \tag{1}$$

with fixed s and varying t, where f is the beat frequency and $\phi_a(s)$, $S_\phi (s)$ and $\phi_b(s)$ are the amplitude, phase and bias of ϕ as functions of s, respectively. The fitting was performed by the method of least squares for arbitrary functions (Bevington and Robinson, 1992). The phase $S_\phi (s)$ was further fitted using equations of the form:

$$S_\phi (s)=S_\phi (0)+(2\pi/\lambda_\phi)s, \tag{2}$$

with varying s, where λ_ϕ is the wavelength of "shear angle wave." The curvature γ (s, t) was also fitted using equations of the form:

$$\gamma (s, t)=\gamma_a(s) \cos \{(S_\gamma(s)-2\pi ft)\}+\gamma_b(s), \tag{3}$$

with fixed s and varying t, where $\gamma_a(s)$, $S_\gamma (s)$ and $\gamma_b(s)$ are the amplitude, phase and bias of γ as functions of s, respectively. The phase $S_\gamma (s)$ was fitted using equations of the form:
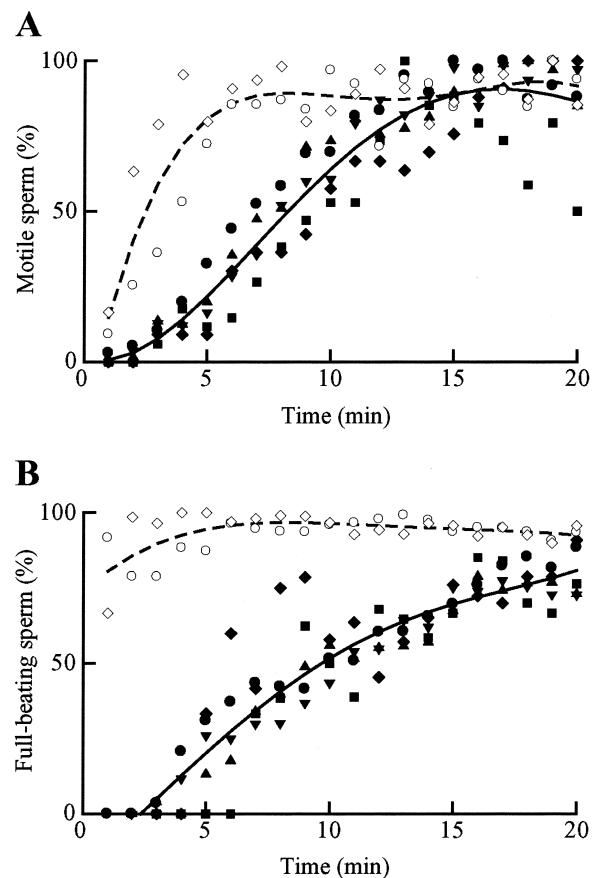

Fig. 1. Motility of sperm of *Hemicentrotus pulcherrimus* after dilution. (A) Motile sperm is expressed as a percentage of all observed in the field of microscope in KEG (five episodes by different closed symbols) and in ASW (two episodes by open). (B) *Full-beating* sperm as a percentage of all motile sperm is plotted for KEG and ASW by the same symbols as used in A, respectively. Lines are curves fitted by the method of least squares using quartic polynomials; T_{M50}=8.3 min (KEG) and 2.5 min (ASW), and T_{F50}=9.8 min (KEG) but not determined for ASW, in which some 80% of motile spermatozoa are already beating to a full extent at the beginning of observation. See text for definitions of T_{M50} and T_{F50}. 20°C.

$$S_\gamma(s)=S_\gamma(0)+(2\pi/\lambda_\gamma)s, \qquad (4)$$

with varying s, where λ_γ is the wavelength of "curvature wave." In the *full-beating* stage, λ_ϕ is generally equal to λ_γ and hence represents the wavelength λ of the bending wave, whereas in the *P-bend propagating* stage λ_ϕ was often much larger than λ_γ because of the absence of R-bend propagation and hence λ_γ, which could also be determined directly by measuring the propagation of the P bend, represents λ. The propagation velocity is given by λf.

To illustrate characteristic features of motility initiation, images were captured, processed to enhance contrast and superimposed by choosing the lightest one for individual pixels using a NEXUS 9000 image processor (Nexus Co., Tokyo).
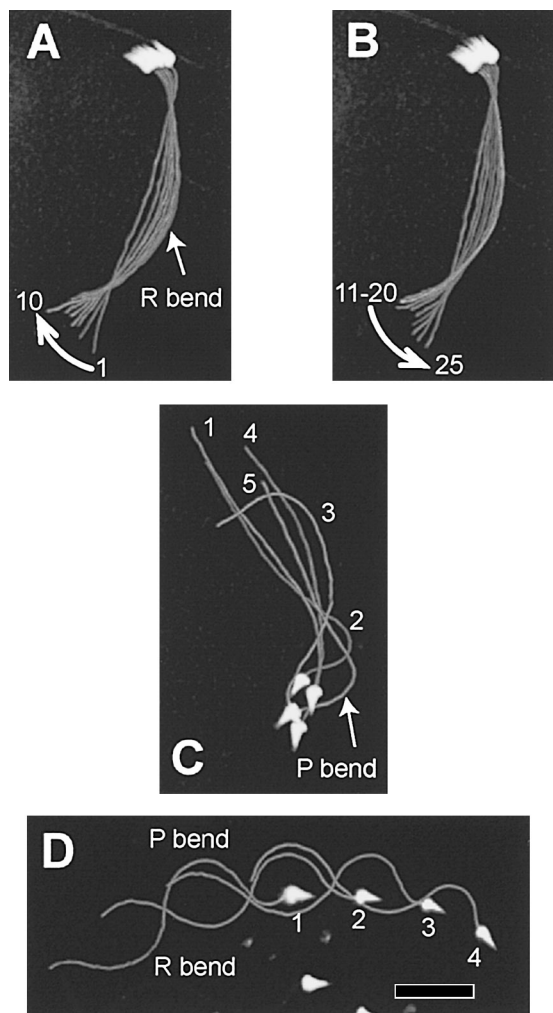
Fig. 2. Bending patterns of sperm of *Hemicentrotus pulcherrimus* after dilution in KEG. Images of a sperm are superimposed at intervals of 1/30 s (VTR). The numbers indicate the sequence of frames. (A, B) C-shaped bending-unbending in the *shivering* stage (5 min 45 s after dilution). A flagellum bends in A (1–10) and unbends in B (20–25), making a standing wave, with a pause in B (11–20). Curved arrows indicate the movement of the flagellar tip. (C) *P-bend propagating* stage (6 min 30 s after dilution). (D) *Full-beating* stage (10 min after dilution). A, B and C are taken from a spermatozoon and D from another. The bend in A and B is identified as R bend as labeled in A and that in C as P bend from images in the *full-beating* stage of that spermatozoon. Bends in the *full-beating* stage (D) are identified as P bend (of higher curvature) or R bend (of lower curvature) as usual. Scale bar: 10 μm. 23°C.

RESULTS

Retardation of motility initiation

An increasing number of spermatozoa became motile after dilution, but substantially slower in KEG than in ASW (Fig. 1). The retardation effect of KEG was about 6 min when measured as the shift in the time after dilution T_{M50}, at which 50% of spermatozoa became motile (Fig. 1A). The retardation to this degree enabled us to observe the transients of initiation and to discriminate stages of different bending patterns (Fig. 2). Figure 1B shows that the emergence of spermatozoon at the final stage *full-beating* in KEG delays about 10 min later than in ASW, when measured as the shift in the T_{F50}, at which 50% of spermatozoa are in the *full-beating* stage.

Progressive stages of initiation

At the very beginning of initiation transients, a number of spermatozoa in KEG were immotile with a straight or slightly bent form (*immotile* stage). An increasing number of them soon shivered at low amplitude (*shivering* stage, Fig.
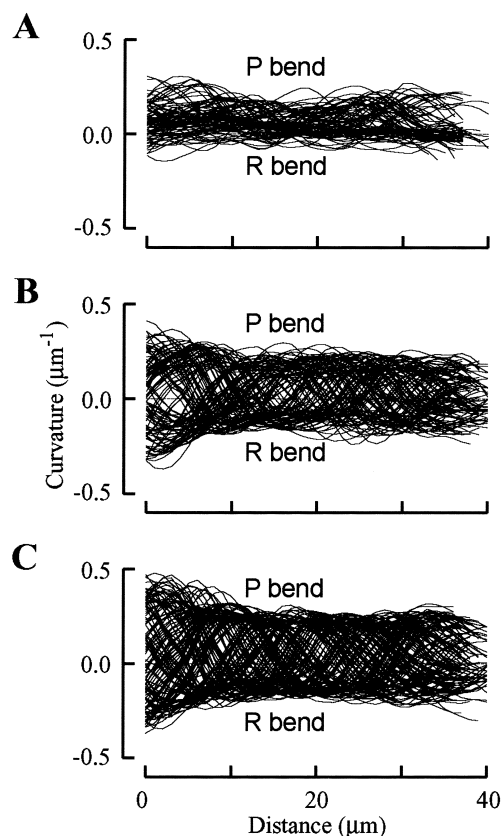
Fig. 3. Curvature profile of sperm of *Hemicentrotus pulcherrimus* in the *P-bend propagating* and *full-beating* stages. The curvature against the distance from the base (1 μm division) is plotted for *P-bend propagating* in KEG (A), *full-beating* in KEG (B) and *full-beating* in ASW (C); the curvature of the P bend is of the positive sign. Randomly sampled waveforms, 79 (A), 108 (B) and 134 (C) in total, are basically from different spermatozoa found by means of mechanical stage scanning. 20°C.

Table 1.   Characteristics of motile spermatozoa after dilution in KEG or ASW.

	P-bend propagating	Full-beating	
	In KEG	In KEG	In ASW
Swimming velocity (μm s^{-1})	75.5±26.9(N=10)	98.0±26.9(N=20)**	158.9±12.8(N=26)
†Amplitude of curvature (μm^{-1})			
P bend	0.13±0.04(N=5)	0.20±0.03(N=13)	0.23±0.03(N=23)
R bend	0.02±0.01(N=5)**	0.14±0.03(N=13)	0.14±0.02(N=23)
†Beat frequency (Hz)	26.0±7.8 (N=5)	39.0±10.5(N=13)*	49.8±5.5 (N=23)
†Amplitude of shear angle (rad)	0.78±0.30(N=5)	0.85±0.12(N=13)	0.92±0.14(N=23)
†Rate of shear angle change (rad s^{-1})	94±40 (N=5)**	206±58 (N=13)**	285±35 (N=23)
†Propagation velocity (mm s^{-1})	1.09±0.35(N=5)	1.08±0.27(N=13)*	1.39±0.28(N=23)
†Wavelength (μm)	44.1±13.1(N=5)	28.2±4.4 (N=13)	27.9±4.5 (N=23)

Values are means±S.D. (N is the number of spermatozoa). An asterisk indicates a significant difference between *P-bend propagating* and *full-beating* in KEG and that between *full-beatings* in KEG and in ASW ($P<0.01$; Students *t*-test) and a double asterisk ($P<0.001$). † Values are computed using equations 1 through 4 in the text, either at 15 μm from base (amplitude, frequency and rate) or over the entire length (velocity and wavelength). 20–22°C.

2A, B). The spermatozoon once in the *shivering* stage was usually found to enter into the next stage, in which its flagellum exclusively propagated a highly asymmetrical bend (Fig. 2C), i.e. convex to one side, instead of alternating bends to either side as found in swimming spermatozoa in seawater. This one-side bend will be called the P bend (principal bend), because it had the same polarity as the P bend of *full-beating* spermatozoa as it turned out by follow-up VTR. Thus, the third stage is designated the *P-bend propagating* stage as stated earlier. The spermatozoon then entered into the *full-beating* stage (Fig. 2D), in which its flagellar beating has the same characteristic features as ordinary ones found in ASW. Individual spermatozoa experience these stages with a sporadic and occasionally reversible transition, making a good number of *P-bend propagating* sperm and an increasing number of *full-beating* sperm throughout initiation transients in KEG. In ASW the initiation transients are so rapid that most of beating sperm are identified as *full-beating* sperm although a small number of irregular sperm remained throughout.

Shivering stage

Most of immotile spermatozoa were floating some distance apart from and at an angle to the surface of either the slide or cover so that it was more difficult to get clear images of the initial movement in the *shivering* stage than those in other later stages, in which they were progressively trapped or guided by the surface with their bending planes being parallel to it. The low amplitude and irregularity in the movement also made it difficult to analyze the flagellar movement in this stage.

A series of events, in which one spermatozoon experienced the C-shaped bending in the *shivering* stage and then transition to the *P-bend propagating* stage, were recorded in good focus. This valuable record showed that either bending or unbending occurred simultaneously along the entire

length of the flagellum, i.e., the bending wave was "standing" (Fig. 2A, B). The length of period of one bending cycle varied with an occasional long pause at either a bent or straight position. The flagellum bent only in one direction, mostly uniformly but a sharper bend at the base. The direction of bending was opposite to that of the P bend in the following *P-bend propagating* stage and hence the bend was identified as R bend.
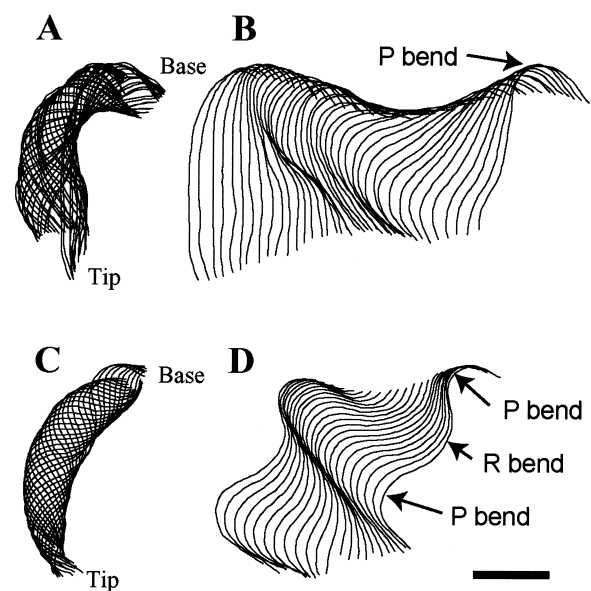

Fig. 4.   Reconstructed bending forms of sperm of *Hemicentrotus pulcherrimus.* Tracings obtained by automatic tracking using flagellar image analysis software, Bohboh, on a PC are superimposed frame by frame at intervals of 1 ms (HSVTR) of one spermatozoon in the *P-bend propagating* stage (A and B) and of another in the *full-beating* stage (C and D). Tracings in B and D are shifted to the right for ease of understanding the wave propagation. Scale bar: 10 μm. 22°C.
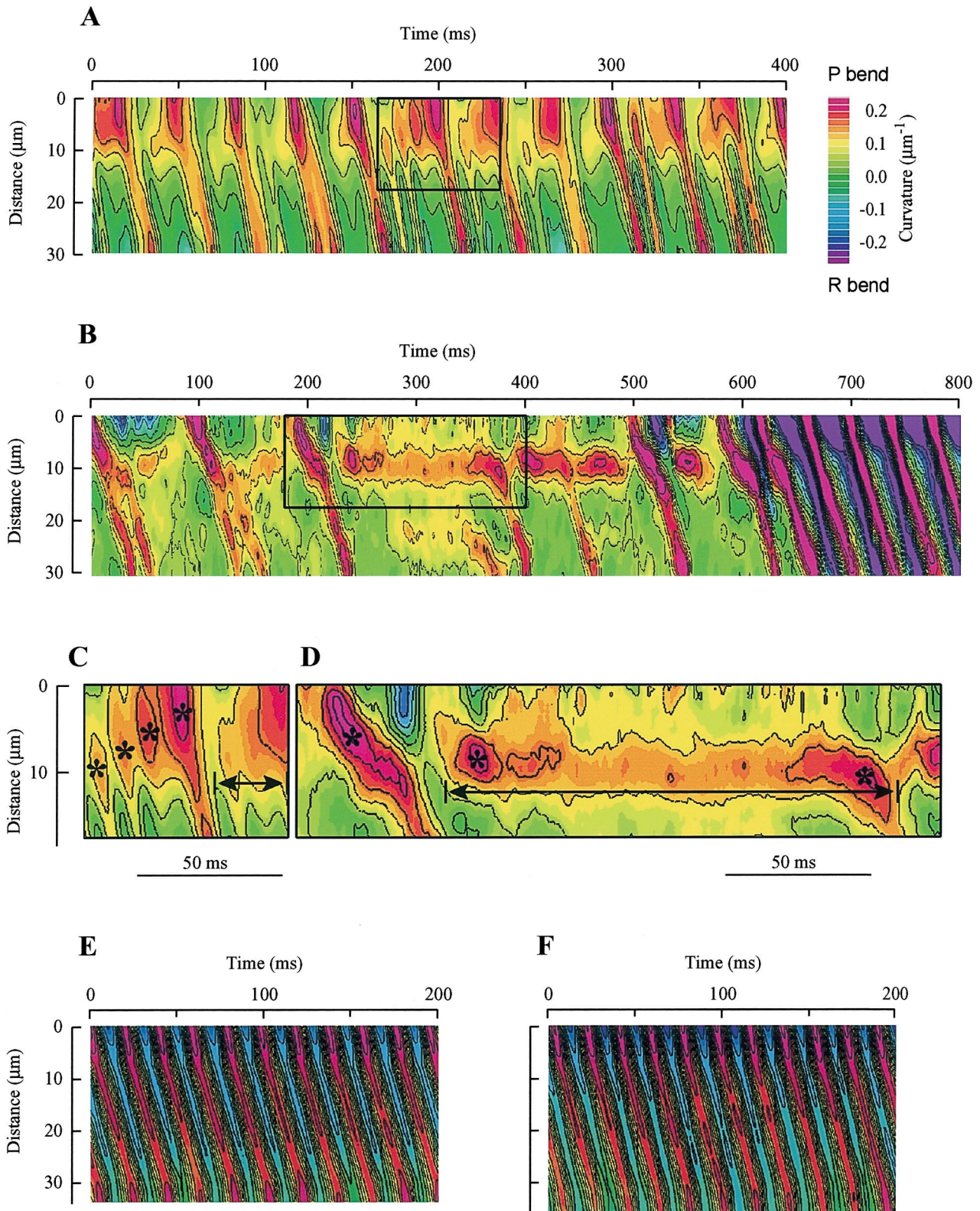
P-bend propagating stage

The curvature of the P bend of the sperm flagella in the *P-bend propagating* stage was only slightly smaller than that in the *full-beating* stage in KEG, which was yet small when compared with that in ASW, while the curvature of the R bend in the *P-bend propagating* stage was substantially smaller than that of the *full-beating* stage (Fig. 3, Table 1). The P bend was generated at the base and propagated
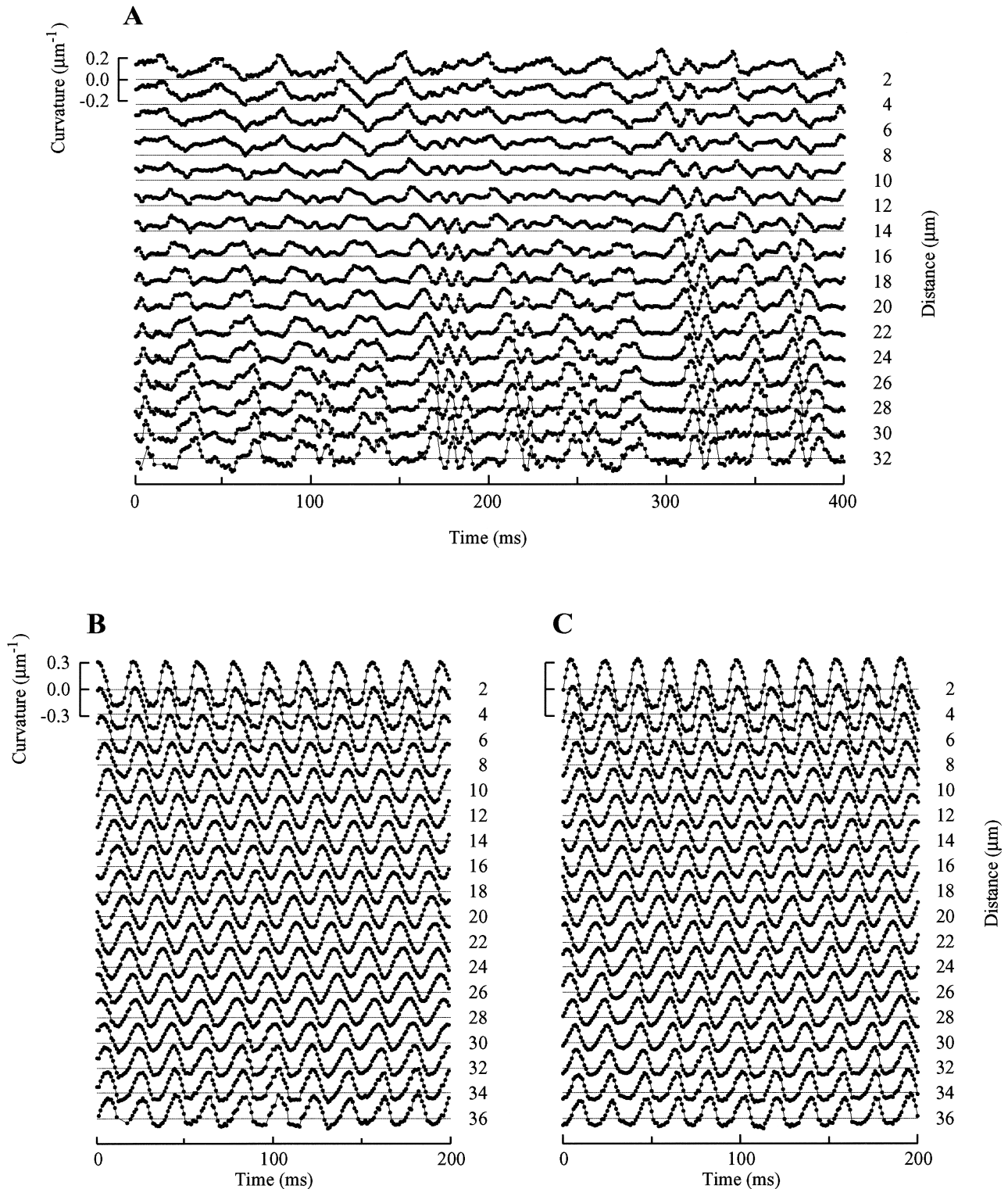
Fig. 5. Curvature of sperm of *Hemicentrotus pulcherrimus*. (A) *P-bend propagating* stage in KEG. (B, C) *full-beating* stage in KEG and ASW, respectively. The curvature is plotted as functions of time (1 ms resolution), at points as indicated by numbers to the right of respective base lines; the curvature of the P bend is of the positive sign. 22°C.

Fig. 6. Pseudocolor-maps of the curvature of sperm of *Hemicentrotus pulcherrimus*. (A–D) *P-bend propagating* stage in KEG, including the transition from the *P-bend propagating* stage to the full-beating in B; enlarged maps of an area indicated by the box in A (C) and of that in B (D). (E, F) *full-beating* stage in KEG and ASW, respectively. Values are encoded in pseudocolor according to the scale shown at the right of the diagram, with colder colors for the R bend and warmer ones for the P bend; contour lines are also given at intervals of 0.05 μm^{-1} division. Asterisks mark the islands of warmer colors and dual-pointing arrows the horizontal bands (see text for islands and bands). A, C, E, F: 22°C, B, D: 16°C.

along the flagellum at a speed, not much different from that in the *full-beating* stage (Figs. 4, 5, Table 1). The generation of the P bend fluctuated in time and site as compared with that of bends in the *full-beating* stage either in KEG or in ASW (Fig. 5); the time and site of bend generation can clearly be expressed by islands and horizontal bands of warmer-color in pseudocolor maps as shown in Fig. 6. The site of bend generation varies along the basal region up to about 10 μm apart from the base (Fig. 6C) and the beginning of propagation is often delayed after the bend is generated (Fig. 6D), whereas both the site and the time are relatively regular in the *full-beating* stage (Fig. 7E, F). The P bend occasionally grew at lower speeds, making the start of propagation rather sporadic in time in the *P-bend propagating* stage than in the *full-beating* stage (Figs. 5, 6). However, once the propagation of the P bend occurred, it was as smooth as that in the *full-beating* stage of either KEG or ASW (compare Fig. 6A, B with Fig. 6E, F). The propagation velocity of this bend was also as large as that in the *full-beating* stage (Table 1). The length of period of one beating cycle varied so much that the beat frequency could not be determined stroboscopically. The fluctuation of beating cycles was also clearly demonstrated by a frame-by-frame

analysis (Figs. 5, 6). The swimming velocity in this stage was about 75% of that in the *full-beating* stage (Table 1). The bending of the flagellum of this stage was still sinusoidal as in the *full-beating* stage, in terms of shear angle as a function of time (Fig. 7), i.e. the wave is approximately "sine-generated" (Hiramoto and Baba, 1978). Thus, the oscillation was considerably symmetric in terms of shear angle when the bias or offset in angle was ignored, and except for irregular pauses at the end of P-bend generating angular change (rising phase in Fig. 7). The rate of angular change in either the P-bend generating direction (rising) or the R-bend generating (falling) was significantly smaller than that of the *full-beating* stage (Fig. 7, Table 1). The bending wave damped along the flagellum when measured by the amplitude of shear angle (Fig. 7), while there was no apparent damping in terms of curvature (Figs. 3, 5).

Full-beating stage

The spermatozoa diluted in KEG swam regularly in the *full-beating* stage with an appearance similar to those activated by dilution in ASW (Figs. 2D, 4C, 4D, 5, 6), although with a little lower beat frequency and lower swimming velocity (Table 1). The bending waves in the *full-beating* stage of
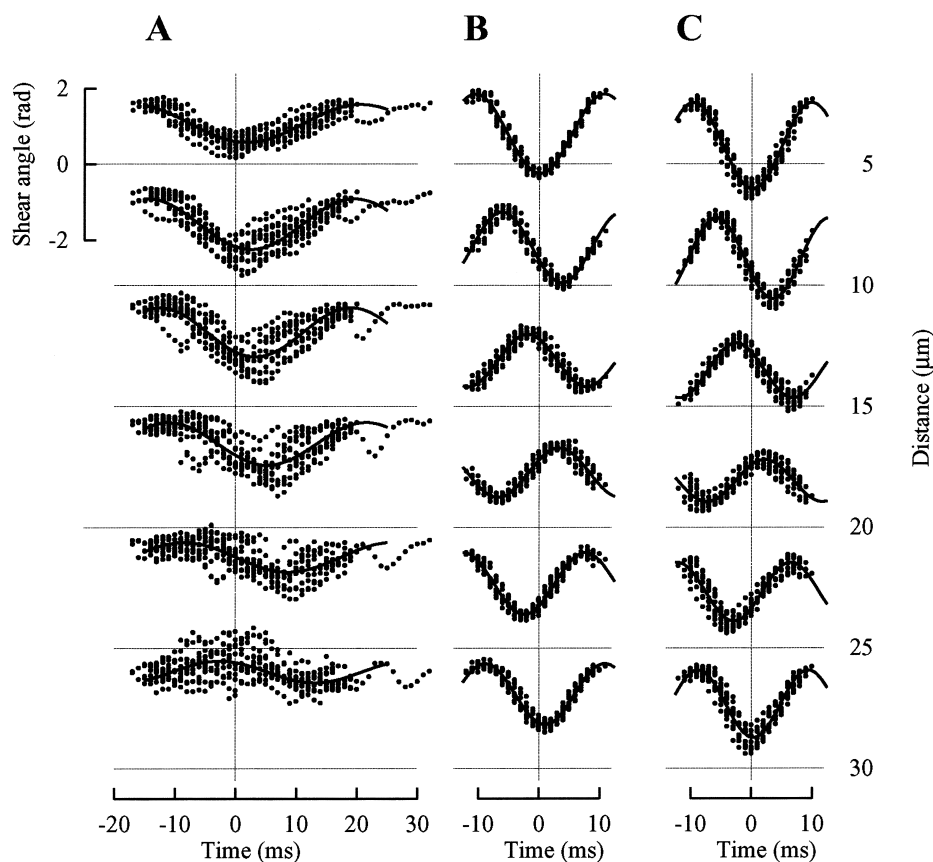
Fig. 7. Shear angle profile of sperm of *Hemicentrotus pulcherrimus*. The shear angle is plotted as functions of time (1 ms resolution) for *P-bend propagating* in KEG (A), *full-beating* in KEG (B) and *full-beating* in ASW (C); the rising phase corresponds to the P bend. Data values have been shifted along the time axis to superpose successive beat cycles (13, 10 and 11 cycles in A, B and C, respectively) into one, by positioning the minimum values for 5 μm in individual cycles to sit at 0 ms on the time axis. Curves are for cosine functions of time, equation 1 in the text, fitted to the shifted values by the methods of least squares. 22°C.

spermatozoa in KEG as well as in ASW were more exactly "sine-generated" than those in the *P-bend propagating* stage in terms of either curvature (Fig. 5) or shear angle (Fig. 7). The P and R bends were generated alternately at a regular position very close to the base at regular time intervals (Fig. 6E, F) as compared with the P bend in the *P-bend propagating* stage, which was often generated at positions substantially distant from the base at rather irregular intervals (Fig. 6A–D). The waves propagated without any discernible damping as of the P bend in the *P-bend propagating* stage in terms of shear angle (Fig. 7).

Transition from *P-bend propagating* to *full-beating*

The spermatozoon in the late *P-bend propagating* stage gradually developed a larger R bend at the base, and eventually entered into the next stage. The images showing the intermediate waveforms between the *P-bend propagating* and *full-beating* stages were seen only in a couple of fields of VTR, indicating that the transition is very momentary. The transition occurred in a short time, within one or two intermediate beating cycles (Fig. 6B). The parameters of bending changed from characteristic values of the *P-bend propagating* stage to those of the *full-beating* stage, which were described earlier under the headings "*P-bend propagating* stage" and "*Full-beating* stage" and summarized in Table 1.

DISCUSSION

Diluting dry sperm of the sea urchin, *Hemicentrotus pulcherrimus,* with KEG instead of ASW delayed the acquisition of motility. This retardation enabled us to observe how individual spermatozoa began their flagellar beating under artificial initiation conditions. The initiation could be divided into four stages: *immotile, shivering, P-bend propagating* and *full-beating*. In the course of natural initiation in ASW, these transitional stages have not yet been confirmed most likely because the initiation can proceed to the final *full-beating* stage before sperm reach the field of observation or because it proceeds through a completely different course of motility acquisition.

Sperm cells are stored in a quiescent state in the gonads, but upon release motility is activated. Activation is triggered by environmental cues through transduction events involving sperm ion channels (Morisawa, 1994; Darszon *et al.*, 1999, 2001). In sea urchins, due to Na^+/H^+ exchange across the sperm plasma membrane, release into seawater is associated with an increase in intracellular pH (pH_i), which, in turn, activates flagellar dynein ATPase (Christen *et al.*, 1982; Schackmann *et al.*, 1984; Lee, 1984a, b). The pH_i is about 6.6 in the quiescent state (Lee, 1984a; Dorsten *et al.*, 1997) and shifts to 7.6 by H^+ extrusion through the Na^+/H^+ exchanger upon activation (Dorsten *et al.*, 1997). The removal of Na^+ in ASW inhibits the sperm motility even if the pH of ASW is as high as the normal level, while the addition of amine can reactivate the motility (Bibring *et al.*, 1984). Since Na^+ is not included in KEG, an

increase of pH_i by the Na^+/H^+ exchange might not occur. It is therefore likely that glycine in KEG enters the cell through anion channels (Darszon *et al.*, 2001) rather than through the Na^+/H^+, elevates the pH_i by neutralization of H^+ in the cell, and triggers the motility as amine does so (Bibring *et al.*, 1984), which is slower than the process by the Na^+/H^+ exchange in ASW under normal conditions.

The dynein ATPase utilizes most of the ATP, which in sea-urchin spermatozoa is delivered exclusively by oxidative phosphorylation in a single mitochondrion located in the midpiece of the sperm cell and is transported most efficiently through the sperm creatine kinase and phosphocreatine system known as the CK/PCr shuttle (Christen *et al.*, 1983). When the CK/PCr shuttle is blocked by specific inhibitors, the flagellar bending waves are rapidly damped as they propagate along the flagellum (Tombes and Shapiro, 1985; Tombes *et al.*, 1987). The fact that there are no significant attenuations in bending waves along the flagellum in KEG indicates that the CK/PCr shuttle is functional during the retarded initiation. The fact that the bending waves in KEG, of either *P-bend propagating* or *full-beating* sperm, have no resemblance with those reported for demembranated sea urchin sperm reactivated at low ATP concentrations, i.e. lower beat frequency and incomplete bend propagation (Gibbons and Gibbons, 1972), also implies an adequate supply of ATP.

It has been shown that ciliary and flagellar motility are regulated by phosphorylation of the axonemal components. With the known exception of carp sperm (Krasznai *et al.*, 2000), phosphorylation on some axonemal proteins by cAMP-dependent kinase is required for initiation of sperm motility including that of sea urchins (Ishiguro *et al.*, 1982; Brokaw, 1984, 1987a; Takahashi *et al.*, 1985; Murofushi *et al.*, 1986; Bracho *et al.*, 1998). It should be noted that cAMP is elevated by 1.9 fold upon dilution from low-pH ASW to Na^+-free, Ca^{2+}-free ASW added with amine (Beltrán *et al.*, 1996), conditions similar to the present. However, the reactivation conditions allow variable levels of motility to be expressed without cAMP incubation, with some species, including *Hemicentrotus*, being already at a high percent motility (Murofushi *et al.*, 1986; Brokaw, 1987a; Bracho *et al.*, 1997).

Demembranated spermatozoa from the tunicate, *Ciona intestinalis*, are immotile in an ordinary "reactivation medium", which has been normally used for sea urchin sperm, and become activated only after incubation with cAMP (Brokaw, 1982, 1987b). Four bending patterns, Patterns C, Q, D and P, appear progressively in the course of cAMP-dependent phosphorylation or reversible dephosphorylation of the axoneme of *Ciona*, and are also found under modified conditions in the sea urchin, *Lytechinus pictus* (Brokaw, 1987b). These patterns have counterparts in the present study. Pattern C appears similar to the C-shaped bending and unbending found in the *shivering* stage. Pattern D is an asymmetric bending pattern and thus appears similar to the bending pattern found in the *P-bend propagating*

stage. There are, however, some significant differences: in Pattern D the bends are damped along the flagellum while they maintain the amplitude unattenuated in the *P-bend propagating* stage; Pattern D accompanies a significant reduction in both wavelength and bend angle, with active bends in both directions at least in the proximal region, while in the *P-bend propagating* stage the P bend has the same characteristic features as the normal beating but with the R bend being almost totally collapsed (Table 1). The limited motility in the *P-bend propagating* stage therefore cannot be due to an incomplete phosphorylation of axonemal components. Pattern P is essentially the same as that of the *full-beating* stage.

It has been shown that an elevated concentration of intracellular Ca^{2+} induces asymmetric beating and quiescence in sea-urchin sperm (Brokaw, 1979; Gibbons and Gibbons, 1980a; Gibbons, 1986). The asymmetrical beating in the *P-bend propagating* stage resembles to this Ca^{2+}-induced asymmetry in that the R bend is reduced in amplitude (Brokaw, 1979; Gibbons and Gibbons, 1980a). There are however substantial differences between these asymmetrical beatings from the following viewpoints: the Ca^{2+}-induced asymmetry does not occur in the Ca^{2+}-free medium as used in the present study (Gibbons and Gibbons, 1980b; Shingyoji and Takahashi, 1995) nor does the intracellular Ca^{2+} concentration elevate when sperm are diluted in Na^+-free, Ca^{2+}-free ASW (Beltrán *et al.*, 1996); the asymmetry in the *P-bend propagating* stage is due to the selective elimination of the R bend as most clearly shown in Fig. 3 while the Ca^{2+}-induced asymmetry is due to an increase in the P bend compensated by a decrease in the R bend, so that there is no change in mean bend angle, as most nicely explained by "biased baseline" mechanism (Brokaw, 1979; Eshel and Brokaw, 1987).

It has been demonstrated that both live and reactivated sea urchin sperm are straightened at low pH and begin to beat asymmetrically, as the pH of medium is increased (Goldstein, 1979). The bending pattern of this asymmetric motion during pH rise is very similar to that in the *P-bend propagating* stage during motility initiation. It has been reported that the P bend of the asymmetric beating of live sperm at intermediate pH attains a speed of about one-third of that attained during steady state beating, while the initial bend, which could not be identified as P or R, of reactivated sperm often attains a speed of propagation similar to those of steady-state bends at pH 8.0; the beat frequency of reactivated sperm at intermediate pH is about one-third of that at pH 8.0, while it has not been measured with live sperm (Goldstein, 1979). Thus, our data that there is no significant difference in speed of the P bend between the *P-bend propagating* and *full-beating* stage irrespective of irregularity of and reduction in beat frequency (Table 1) may represent more accurately the nature of bending, probably at different pH. The R bend begins to develop later as the pH is increased further (Goldstein, 1979), which may corresponds to the transition from the *P-bend propagating* to *full-beating*

stage. The asymmetrical beating of this type has also been found during the stopping transients upon a rapid drop in the pH of reactivation medium (Sato *et al.*, 1988). It is therefore likely that *P-bend propagating* bends are generated under intermediate conditions made in the course of gradual increase in the intracellular pH. It has been demonstrated that one of potentially alternating bends propagates with the other being collapsed during the trypsin digestion in the presence of CO_2 (Brokaw and Simonick, 1977), although the propagating bend has not been identified as P or R. These findings may indicate that the axonemal structures including dynein ATPase have subtle differences in sensitivity to their environmental pH or CO_2, resulting in selective inhibition of specific sliding between adjacent doublets required for bend generation or propagation, since the P and R bends are topographically related to the axonemal structure (Mohri *et al.*, 1987).

The site of generation of the P bend in the *P-bend propagating* stage varies in position in the basal region up to 10 μm, making islands or hot spots clearly some distance apart from the base (Fig. 6), which has not been demonstrated with sperm flagella in the *full-beating* stage nor under other experimental conditions. Goldstein has reported that the development of the first bend near the base (P bend) upon pH rise is accompanied by the formation of a broad, more distal, curve in the opposite direction (R bend) and that this curve occasionally develops into a traveling bend (Fig. 4 of Goldstein, 1979); similar starting transients have been described by tracings of one spermatozoon at normal pH (Fig. 11 of Rikmenspoel, 1978). Thus, our findings indicate more evidently that the ability of autonomous P bend generation at and propagation from a portion of the axoneme is not exclusively possessed by the very basal region but can be unmasked throughout a wider region when the R bend is suppressed.

In conclusion, sea-urchin sperm can selectively propagate the P bend under certain conditions, most likely at low pH. Analyses for components responding to these modified beating remained to be studied.

REFERENCES

Baba SA, Mogami Y (1985) An approach to digital image analysis of bending shapes of eukaryotic flagella and cilia. Cell Motil 5: 475–489

Baba SA, Mogami Y (1987a) High time-resolution analysis of transient beating patterns during ciliary responses following electric stimulation in sea urchin embryos. Cell Motil Cytoskeleton 7: 198–208

Baba SA, Mogami Y (1987b) Device for controlled intensification of the light output of xenon flash tubes. Rev Sci Instrum 58: 1312-1313

Beltrán C, Zapata O, Darszon A (1996) Membrane potential regulates sea urchin sperm adenylylcyclase. Biochemistry 11: 7591–7598

Bevington PR, Robinson D (1992) Data Reduction and Error Analysis for The Physical Sciences. 2nd Ed, McGraw-Hill, New York

Bibring T, Baxbandall J, Harter CC (1984) Sodium-dependent pH

regulation in active sea urchin sperm. Dev Biol 101: 425–435

Bracho GE, Fritch JJ, Tash JS (1997) A method for preparation, storage, and activation of large populations of immotile sea urchin sperm. Biochem Biophys Res Commun 237: 59–62

Bracho GE, Fritch JJ, Tash JS (1998) Identification of flagellar proteins that initiate the activation of sperm motility *in vivo*. Biochem Biophys Res Commun 242: 231–237

Brokaw CJ (1979) Calcium-induced asymmetrical beating of triton-demembranated sea urchin sperm flagella. J Cell Biol 82: 401–411

Brokaw CJ (1982) Activation and reactivation of *Ciona* spermatozoa. Prog Clin Biol Res 80: 185–189

Brokaw CJ (1984) Cyclic AMP-dependent activation of sea urchin and tunicate sperm motility. Ann NY Acad Sci 438: 132–141

Brokaw CJ (1987a) A lithium-sensitive regulator of sperm flagellar oscillation is activated by cAMP-dependent phosphorylation. J Cell Biol 105: 1789–1798

Brokaw CJ (1987b) Regulation of sperm flagellar motility by calcium and cAMP-dependent phosphorylation. J Cell Biochem 35: 175–184

Brokaw CJ, Simonick TF (1977) Motility of triton-demembranated sea urchin sperm flagella during digestion by trypsin. J Cell Biol 75: 650–665

Christen R, Schackmann RW, Shapiro BM (1982) Elevation of the intracellular pH activates respiration and motility of sperm of the sea urchin, *Strongylocentrotus purpuratus*. J Biol Chem 257: 14881–14890

Christen R, Schackmann RW, Shapiro BM (1983) Metabolism of sea urchin sperm. Interrelationships between intracellular pH, ATPase activity, and mitochondrial respiration. J Biol Chem 258: 5392–5399

Christen R, Schackmann RW, Shapiro BM (1986) Ionic regulation of sea urchin sperm motility, metabolism and fertilizing capacity. J Physiol 379: 347–365

Clapper DL, Davis JA, Lamothe PJ, Patton C, Epel D (1985) Involvement of zinc in the regulation of pHi, motility, and acrosome reactions in sea urchin sperm. J Cell Biol 100: 1817–1824

Darszon A, Labarca P, Nishigaki T, and Espinosa F (1999) Ion channels in sperm physiology. Physiol Rev 79: 481–510

Darszon A, Beltrán C, Felix R, Nishigaki T, Trevino CL (2001) Ion transport in sperm signaling. Dev Biol 240: 1–14

Dorsten FA van, Wyss M, Wallimann T, Nicolay K (1997) Activation of sea-urchin sperm motility is accompanied by an increase in the creatine kinase exchange flux. Biochem J 325: 411–416

Eshel D, Brokaw CJ (1987) New evidence for a "biased baseline" mechanism for calcium-regulated asymmetry of flagellar bending. Cell Motil Cytoskeleton 7: 160–168

Gatti JL, Christen R (1985) Regulation of internal pH of sea urchin sperm. A role for the Na/K pump. J Biol Chem 260: 7599–7602

Gibbons BH, Gibbons IR (1972) Flagellar movement and adenosine triphosphatase activity in sea urchin sperm extracted with Triton X-100. J Cell Biol 54: 75–97

Gibbons BH, Gibbons IR (1980a) Calcium-induced quiescence in reactivated sea urchin sperm. J Cell Sci 84: 13–27

Gibbons IR, Gibbons BH (1980b) Transient flagellar waveforms during intermittent swimming in sea urchin sperm. I. Wave parameters. J Muscle Res Cell Motil 1: 31–59

Gibbons IR (1986) Transient flagellar waveforms in reactivated sea urchin sperm. J Muscle Res Cell Motil 7: 245–250

Goldstein SF (1979) Starting transients in sea urchin sperm flagella. J Cell Biol 80: 61–68

Hiramoto Y, Baba SA (1978) A quantitative analysis of flagellar movement in echinoderm spermatozoa. J Exp Biol 76: 85–108

Ishiguro K, Murofushi H, Sakai H (1982) Evidence that cAMP-dependent protein kinase and a protein factor are involved in reactivation of Triton X-100 models of sea urchin and starfish spermatozoa. J Cell Biol 92: 777–782

Krasznai Z, Marian T, Izumi H, Damjanovich S, Balkay L, Tron L, Morisawa M (2000) Membrane hyperpolarization removes inactivation of Ca^{2+} channels, leading to Ca^{2+} influx and subsequent initiation of sperm motility in the common carp. Proc Natl Acad Sci USA 97: 2052–2057

Lee HC (1984a) Sodium and proton transport in flagella isolated from sea urchin spermatozoa. J Biol Chem 259: 4957–4963

Lee HC (1984b) A membrane potential-sensitive Na+-H+ exchange system in flagella isolated from sea urchin spermatozoa. J Biol Chem 259: 15315–15319

Lee HC, Johnson C, Epel D (1983) Changes in internal pH associated with initiation of motility and acrosome reaction of sea urchin sperm. Dev Biol 95: 31–45

Miller RL, Brokaw CJ (1970) Chemotactic turning behaviour of Tubularia spermatozoa. J Exp Biol 52: 699–706

Miyake MO, Mogami Y, Kataoka E, Kajita E, Baba SA (1998) Improvement in time and space resolution of stroboscopic micrography using high power xenon flash. Rev Sci Instrum 69: 325–326

Mohri H, Mohri T, Okuno M (1987) Topographical relationship between the axonemal arrangement and the bend direction in starfish sperm flagella. Cell Motil Cytoskeleton 8: 76–84

Morisawa M (1994) Cell signaling mechanisms for sperm motility. Zool Sci 11: 647–662

Murofushi H, Ishiguro K, Takahashi D, Ikeda J, Sakai H (1986) Regulation of sperm flagellar movement by protein phosphorylation and dephosphorylation. Cell Motil Cytoskeleton 6: 83–88

Rikmenspoel R (1978) Movement of sea urchin sperm flagella. J Cell Biol 76: 310–322

Sato F, Mogami Y, Baba SA (1988) Flagellar quiescence and transience of inactivation induced by rapid pH drop. Cell Motil Cytoskeleton 10: 374–379

Schackmann RW, Christen R, Shapiro BM (1984) Measurement of plasma membrane and mitochondrial potentials in sea urchin sperm. Changes upon activation and induction of the acrosome reaction. J Biol Chem 259: 13914–13922

Shingyoji C, Takahashi K (1995) Flagellar quiescence response in sea urchin sperm induced by electric stimulation. Cell Motil Cytoskeleton 31: 59–65

Takahashi D, Murofushi H, Ishiguro K, Ikeda J, Sakai H (1985) Phosphoprotein phosphatase inhibits flagellar movement of Triton models of sea urchin spermatozoa. Cell Struct Funct 10: 327–337

Tombes RM, Shapiro BM (1985) Metabolite channeling: a phosphorylcreatine shuttle to mediate high energy phosphate transport between sperm mitochondrion and tail. Cell 41: 325–334

Tombes RM, Brokaw CJ, Shapiro BM (1987) Creatine kinase-dependent energy transport in sea urchin spermatozoa. Flagellar wave attenuation and theoretical analysis of high energy phosphate diffusion. Biophys J 52: 75–86